AIAA SciTech Forum
7-11 January 2019, San Diego, California
AIAA Scitech 2019 Forum

10.2514/6.2019-0465

Time-Resolved Electron Temperature and Species Measurements and Predictions of Plasma-Assisted Reforming of Methane

Timothy Y. Chen[1], Suo Yang[2], Aric C. Rousso[3], Benjamin M. Goldberg[4], Shuqun Wu[5], Egemen Kolemen[6], and Yiguang Ju[7]
[1,3-7]*Department of Mechanical and Aerospace Engineering, Princeton University, Princeton, NJ 08544*
[2]*Department of Mechanical Engineering, University of Minnesota, Minneapolis, MN 55455*
[5]*Center for More Electric Aircraft Power System, College of Automation Engineering, Nanjing University of Aeronautics and Astronautics, Nanjing, Jiangsu 210016, China*

I. Introduction

Low-temperature plasmas present a promising alternative to large reforming facilities as a method for processing excess methane to reduce emissions from gas flaring. The Global Gas Flaring Reduction Partnership reported that 143 billion cubic meters of gas was flared in 2016, equivalent to 4% of global production of natural gas that year [1, 2]. Gas flaring contributes up to 1% of global annual carbon dioxide emissions and produces black carbon which is a powerful driver of climate change [3, 4]. Thus, plasma processing of methane together with carbon dioxide is important from an environmental standpoint and has been an area of interest for the past several decades [5, 6].

Recently, it has been shown that dry reforming of methane in plasma discharges can produce value-added products such as formaldehyde and methanol [7, 8]. Wang *et al.* [7] showed that it was possible to dry reform methane into liquid products in one step by pairing catalysts in a cooled plasma reactor. Typically, these experimental studies follow a trial-and-error approach and study the effects of varying process parameters such as types of catalysts and mixture composition. However, to make plasmas viable for industrial use, a predictive model is needed to efficiently optimize the selectivity toward desired products and to increase the energy conversion efficiency.

Currently, the key reaction pathways of plasma-assisted fuel reforming are not well understood, even without including catalysts. Plasma chemistry models are validated by gas chromatography (GC) due to a lack of time-resolved measurements in the literature [9-11]. It has been shown that while plasma chemistry models can predict major species (e.g. CO, H_2O, CH_4), significant discrepancy between measured and predicted intermediate species such as formaldehyde can exist [12-14]. In an n-heptane oxidation study, Rousso *et al.* [13] found a forty times difference between the predicted and measured formaldehyde, while for methane oxidation, Lefkowitz *et al.* [12] saw an underprediction of four times. One stated reason for the discrepancy is that formaldehyde and methanol concentrations are sensitive to the branching ratio of the reaction between fuel and $O(^1D)$. *In-situ* time-resolved laser diagnostics are therefore needed to find critical areas of uncertainty in the plasma chemistry models so that they can be improved.

In addition, according to the work from Yang *et al.* [15], after detailed comparison between numerical results from 1-D model and 0-D model of plasma-assisted fuel pyrolysis and oxidation, it shows that 1-D model has a much better agreement with experimental results. In the 0-D models, plasma discharges are set to be uniform for the entire domain during each voltage pulse, without taking into consideration cathode sheath formation, accumulation on the dielectric layers, and species/heat diffusion effects. In addition, the reduced electric field (E/N) and electron number density charge are pre-specified rather than calculated. Together these assumptions create inaccuracies which increase the mismatch between the model and the experimental results. This 1-D model has also been successfully applied to investigate plasma assisted ignition of H_2-air mixtures and dimethyl ether (DME) /O_2/Ar mixtures[16, 17]. Therefore, the 1-D model is expected to also be very useful for plasma assisted fuel reforming.

---

[1] Ph.D. Candidate, tc8@princeton.edu, Student Member AIAA.
[2] Richard & Barbara Nelson Assistant Professor, Member AIAA.
[3] Ph.D. Candidate, Student Member AIAA.
[4] Postdoctoral Research Associate, Member, AIAA
[5] Visiting Scholar, Associate Professor.
[6] Assistant Professor.
[7] Robert Porter Patterson Professor, Associate Fellow AIAA.

In this study, species concentrations will be measured in a 15%/15%/70% CH_4/CO_2/He nanosecond-pulsed plasma. Using laser absorption spectroscopy, this data will serve as validation targets for a 1D model studying the addition of CO_2. Additionally, Thomson scattering will be used to measure the time-resolved electron temperature and number density of CH_4/He mixtures to validate the plasma kinetics involving CH_4 addition to He. Thomson Scattering is a non-intrusive diagnostic that uses Doppler-broadened light scattering from electrons to infer the electron temperature and number density [18, 19]. Thomson Scattering can serve as validation for the 1-D model as the model calculates the electric field through Poisson's equation of electric potential, which in turn influences the predicted electron temporal dynamics. This data will be used to further develop models equipped with detailed plasma chemistry kinetics.

II. Experimental Methods

The experimental apparatus has been described in previous studies and has been presented in previous publications [12, 13, 20].The flow reactor consists of a plane-to-plane dielectric barrier discharge with 44.5 mm square metal electrodes. The pressure is maintained at 60 Torr and the flow velocity is 0.2 m/s. The nanosecond pulses are generated using an FID GmBH FPG 30-50MC4 power supply with a repetition frequency of 30 kHz, FWHM of 12 ns, and peak voltage capability of 32 kV. The power supply is triggered using an SRS DS345 function generator in a burst mode with a burst frequency of 1 Hz to guarantee fresh gas in the measurement volume. Each burst consists of 600 pulses with a pulse repetition frequency of 30 kHz. An external-cavity quantum cascade laser (EC-QCL) from Daylight Solutions (21074-MHF) is used to scan CH_4, C_2H_2, and H_2O absorption lines. The C_2H_2 line is located at 1321.03 cm^{-1}. CH_4 absorption lines at 1343.56 cm^{-1} and 1343.63 cm^{-1} were used for the two-line temperature measurement described by Farooq et al. [21]. A distributed feedback quantum cascade laser (DFB QCL) from Alpes Lasers (sbcw3176) is used to measure CH_2O at 1726.9 cm^{-1}. Lastly, a DFB QCL from Nanoplus (DFB-260290) is used to monitor CO_2 at 3565.33 cm^{-1}. Each laser enters a 24-pass Herriott cell in the flow reactor before reaching the detector. A Tektronix DPO7104C oscilloscope is used to save the collected data. All laser absorption data is processed by fitting simulated spectra using the HITRAN database [20, 22]. A 50.8 mm germanium etalon is used to determine the frequency axis for the collected spectra.

A new experimental setup for the Thomson scattering diagnostic has been built and shown in Fig. 1. A 10 Hz frequency-doubled Quantel Q-Smart 850 Nd:YAG laser is focused to the center of the plasma reactor by an anti-reflection coated (AR coated) plano-convex lens (L1) with a focal length of 1.4 m. The center of the reactor is quartz made to match the electrode geometry and gap distance of the plasma reactor used in the laser absorption measurements. A pair of 1-inch diameter AR coated achromatic lenses of focal length 150mm (L2 and L3) collects the scattered light and focuses it into an f/6.5 Acton SpectraPro 2500i spectrometer. The scattered light is rotated by an image rotator which is made up of two mirrors in a periscope configuration and two more mirrors to match the height of the mirrors with the spectrometer slit. Slit widths of 150 um are used, and a 2400 grooves/mm holographic grating optimized for visible light disperses the light. Thomson spectra are resolved by placing a blackened mask at the spectrometer focal plane. This physically blocks the Rayleigh scattering at 532 nm, which allows for high intensifier gain and long on-chip charge coupled device (CCD) accumulations without saturating the camera. A Princeton Instruments PIMAX 1300 intensified CCD (ICCD) camera with a UNIGEN II filmless intensifier is used to detect the signal photons. An SRS DG535 delay generator is used to trigger the Nd:YAG laser, ICCD, and an SRS DG645 digital delay/pulse generator. The DG645 is used to send the plasma pulse trigger and has a low jitter of around 20 ps. The SRS DS345 used previously in the laser absorption measurements had too large of a jitter for the Thomson Scattering diagnostic. The laser pulse energy is measured periodically using an Ophir PE50BF-DIF-C pyroelectric energy sensor. Stray light, plasma emission, and dark current spectra are measured to subtract out any interfering signals. Absolute number density calibration is done using Raman Scattering in N_2 at 60 Torr. Each Thomson spectrum is fit with a Gaussian profile to determine electron temperature, and the area under this Gaussian is integrated to infer the electron number density.

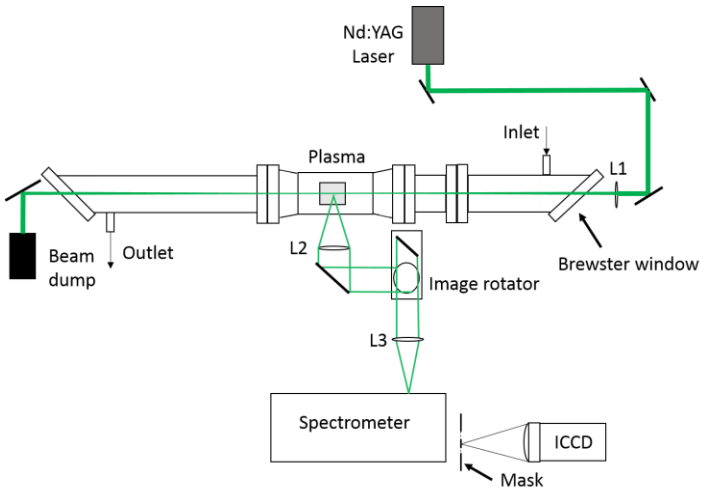

Figure 1. Thomson Scattering experimental setup.

III. Numerical Methods

The 1-D model is adopted from Yang *et al.* [23, 24]. The physical configuration of the plane-to-plane dielectric barrier discharge is shown in Fig. 3a with the 1-D simulation domain being marked as a dashed line. In this work, the computational domain is set to be from the left electrode to the right electrode, with the right electrode connecting to a high voltage power supply, and the left electrode being grounded. Each electrode is covered with dielectric layers, with the gas mixture filling the gap between dielectrics. The dielectric constants are fixed for all simulations in the present work. Gaussian voltage pulses fitted from the experimental measurement of applied voltage (Vapp) are applied, as shown in Fig. 3b. Governing equations include the equation of electric potential, equation of electron energy, transport equations of both charged and neutral species, and conservation equations for mass, momentum, and energy of the gas mixture, and are solved simultaneously to model the flow motions. In particular, by solving the 1-D Poisson equation of electric potential, the breakdown of the gas mixture can be accurately captured as the sharp drop of gap voltage (Vgap) in Fig. 3b. In addition to the electron-impact reaction rate coefficients, the electron transport coefficients are also expressed as functions of electron energy by BOLSIG [25], and are updated through interpolation for every time-step. The plasma drift-diffusion fluid model with the 'local electron mean energy approximation' is applied for the transport of plasma species and energy [26].

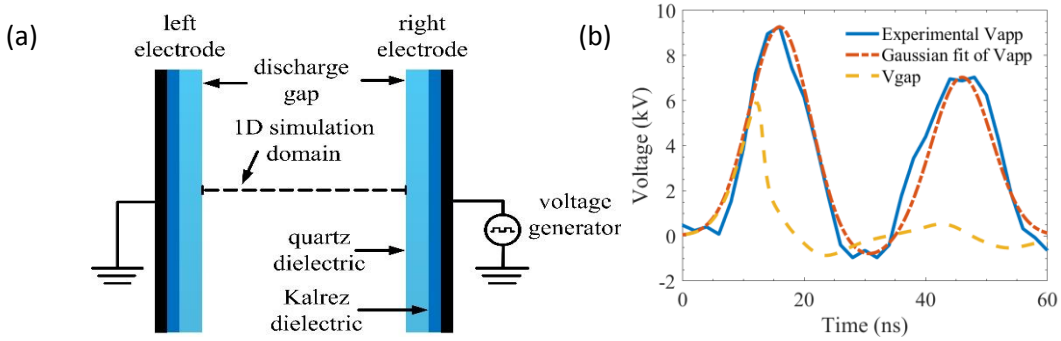

Figure 3. (a) Schematic of physical configuration of the 1-D simulation and (b) Gaussian fit of experimental pulse waveform of applied voltage (Vapp) used in simulation and the resulting gap voltage (Vgap)

Wang et al. [27] was used as the base mechanism for the chemical kinetics in the 1-D model, and the Helium mechanism was updated with additional reactions from [28]. To speed up computation time, the kinetic mechanisms were reduced by removing species such as O_2 and O_3 and several electron-impact processes such as vibrational excitation of CH_4.

IV. Results and Discussion

The electron number density and temperature has been measured in a CH_4/He discharge at 60 Torr with CH_4 addition varying from 0 to 2%. The plasma was run continuously at 100 Hz with a flow speed of 1.26 m/s. This approximates a single pulse measurement, as the electron number density and temperature decays sufficiently (i.e., negligible electron number density, and electron temperature as low as the gas temperature) within the 10 ms inter-pulse period. Five to six frames with 2-3000 accumulations per spectrum were averaged to achieve the required signal to noise ratio. The laser pulse energy for this set of data was 230 mJ/ pulse. The experimental electron number density and temperature are plotted together with the model predictions in Fig. 4.

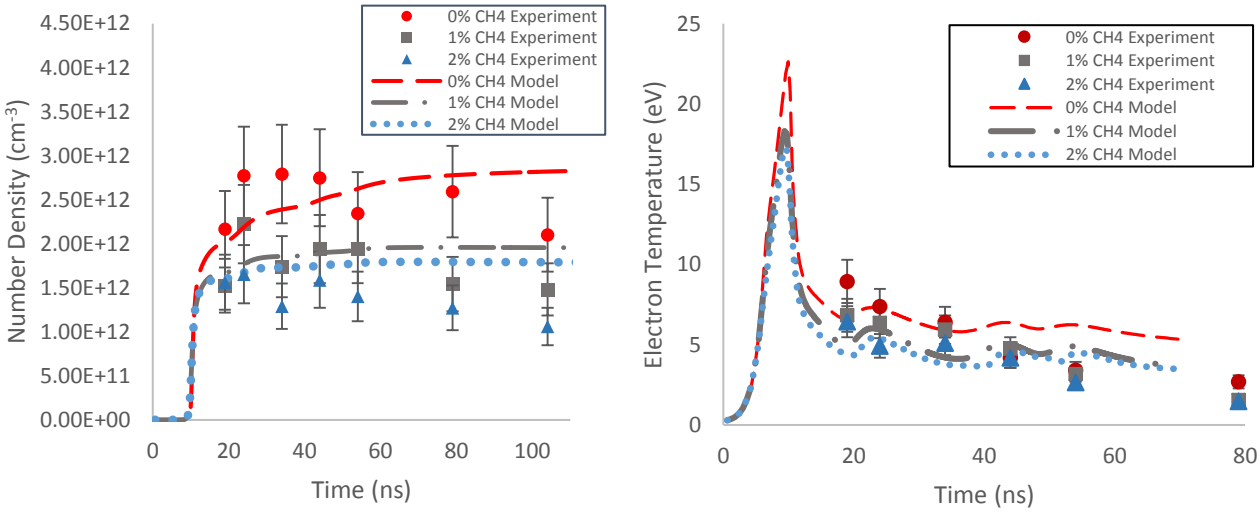

Figure 4. Time resolved electron number density and temperature measurements and model predictions.

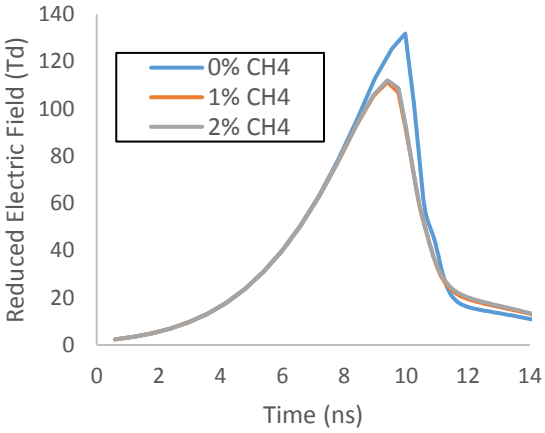

Figure 5. Temporal evolution of E/N during a nanosecond voltage pulse for the 0-2% CH_4 addition mixtures (predicted by the model).

From Fig.4, the overall magnitude of the electron number density and temperature are well predicted by the model. However, the decays of both electron number density and temperature in the experiment were faster than those in the model. For the electron number density, there could be missing recombination pathways in the kinetic mechanism that would accelerate the electron number density decay. The electron temperature decay could be accelerated by including more electron-impact cross-sections. For example, vibrational excitation and excitation of He to electronic states higher than He(^{2}1S) were not considered in this computation. Interestingly, the model does

predict the relative difference in electron temperature between the three experimental conditions. That is, adding 1% CH_4 induces a significant decrease in electron temperature, but adding 2% CH_4 does not show a similarly large decrease in electron temperature. By around 80ns, the 1% and 2% CH_4 mixtures decay to the about the same electron temperature, while at same point in time, the 0% CH_4 mixture is 1 eV hotter. Since electron temperature is primarily governed by the reduced electric field (E/N), the E/N curves for the three mixtures (predicted by the model) were plotted in Fig. 5. The E/N for 0% CH_4 has a larger primary spike in reduced electric field than the 1% and 2% CH_4 mixtures. Furthermore, the E/N is almost the same for the 1% and 2% CH_4 mixtures. We can infer from this plot that the breakdown voltage must be lower with CH_4 addition. The ionization potential of CH_4 is about half of that of He, so the overall breakdown voltage would decrease. But the effect is saturated from 1% to 2% of CH_4 addition.

Time-resolved CH_2O concentration presented in Fig. 6 was measured in a 15% CH_4, 15% CO_2, 70% He mixture using laser absorption. The applied voltage setting was kept the same between the CH_4/He and CH_4/CO_2/He experiments. 600 voltage pulses were applied at 30 kHz. The uncertainty was estimated to be 10% for the CH_2O measurement. The corresponding simulation data is not available yet, and it will be compared to the experimental data in our later presentation and publication.

Across the 600-pulse burst, CH_2O production was observed, where it increased in concentration during the discharge and remained constant afterward. This suggests that its production and consumption is entirely governed by the discharge and not any subsequent chemistry afterward. In other words, there exists a possibility to optimize for these products by changing the plasma parameters such as voltage or pulse repetition rate. More detailed information will be provided later by the pathway flux analysis based on the simulation data.

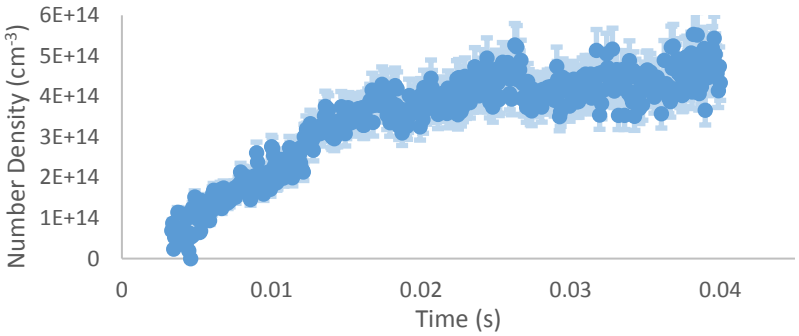

Figure 6. CH_2O time-resolved species concentration profile.

V. Conclusions

The electron temperature and number density were measured for CH_4/He nanosecond-pulsed plasma mixtures ranging from 0 to 2% CH_4 addition. The electron temperature and number density were predicted using a 1-D simulation with a reduced plasma kinetics set. The overall magnitude of both the electron temperature and number density correspond well, but the decays of both were predicted to be too slow. Missing recombination pathways in the kinetic mechanism and electron-impact cross-sections could be the reasons for this discrepancy. Furthermore, the model does predict the significant decrease in electron temperature by adding 1% CH_4 and the marginal decrease by adding 2% CH_4 to the discharge. Plotting the E/N shows that the E/N for the 0% is distinctly higher than the 1% CH_4 case, while the E/N for the 1% CH_4 and 2% CH_4 cases were almost the same. We can conclude that this effect can be attributed to the lowering of the breakdown voltage from addition of CH_4, as the ionization potential for CH_4 is about half of that of He. But the lowering has its limit, and it saturates from 1% to 2% CH_4 addition.

CH_2O concentrations were measured in a 15%/15%/70% CH_4/CO_2/He nanosecond-pulsed plasma in a burst of 600 pulses at 30 kHz frequency. It was shown that CH_2O was formed during the discharge, and its concentrations were constant afterward. Therefore, the plasma entirely governs their consumption and formation processes, which enables the possibility for optimizing the selectivity of these species through plasma parameters such as the voltage pulse frequency. For future work, 1-D simulations of this discharge will be conducted to understand the reaction pathways of plasma-assisted fuel reforming and to study the effect of manipulating the plasma parameters.

Acknowledgement

This work was supported by ExxonMobil through its membership in the Princeton E-filliates Partnership of the Andlinger Center for Energy and the Environment. The authors would also like to acknowledge the ONR STTR, whose support provided funding for this research area. TYC is partially supported through the Program in Plasma Science and Technology at Princeton University Fellowship.

References

[1] Partnership, G. G. F. R., "Gas flaring data 2013-2016." The World Bank, 2017.

[2] BP. "BP Statistical Review of World Energy." 2017.

[3] Boden, T. A., G. Marland, and R.J. Andres. "Global, Regional, and National Fossil-Fuel CO2 Emissions. ." Oak Ridge National Laboratory, Oak Ridge, Tennessee, 2017.

[4] Huang, K., and Fu, J. S., "A global gas flaring black carbon emission rate dataset from 1994 to 2012," *Scientific Data*, Vol. 3, 2016, p. 160104. doi: 10.1038/sdata.2016.104

[5] Scapinello, M., Delikonstantis, E., and Stefanidis, G. D., "The panorama of plasma-assisted non-oxidative methane reforming," *Chemical Engineering and Processing: Process Intensification*, Vol. 117, 2017, pp. 120-140. doi: 10.1016/j.cep.2017.03.024

[6] Zhou, L. M., Xue, B., Kogelschatz, U., and Eliasson, B., "Nonequilibrium Plasma Reforming of Greenhouse Gases to Synthesis Gas," *Energy & Fuels*, Vol. 12, No. 6, 1998, pp. 1191-1199. doi: 10.1021/ef980044h

[7] Wang, L., Yi, Y., Wu, C., Guo, H., and Tu, X., "One-Step Reforming of CO2 and CH4 into High-Value Liquid Chemicals and Fuels at Room Temperature by Plasma-Driven Catalysis," *Angew Chem Int Ed Engl*, Vol. 56, No. 44, 2017, pp. 13679-13683. doi: 10.1002/anie.201707131

[8] Indarto, A., "A review of direct methane conversion to methanol by dielectric barrier discharge," *IEEE Transactions on Dielectrics and Electrical Insulation*, Vol. 15, No. 4, 2008.

[9] Bogaerts, A., De Bie, C., Snoeckx, R., and Kozák, T., "Plasma based CO2 and CH4 conversion: A modeling perspective," *Plasma Processes and Polymers*, Vol. 14, No. 6, 2017. doi: 10.1002/ppap.201600070

[10] Snoeckx, R., Aerts, R., Tu, X., and Bogaerts, A., "Plasma-Based Dry Reforming: A Computational Study Ranging from the Nanoseconds to Seconds Time Scale," *The Journal of Physical Chemistry C*, Vol. 117, No. 10, 2013, pp. 4957-4970. doi: 10.1021/jp311912b

[11] Wang, W., Snoeckx, R., Zhang, X., Cha, M. S., and Bogaerts, A., "Modeling Plasma-based CO2 and CH4 Conversion in Mixtures with N2, O2, and H2O: The Bigger Plasma Chemistry Picture," *The Journal of Physical Chemistry C*, Vol. 122, No. 16, 2018, pp. 8704-8723. doi: 10.1021/acs.jpcc.7b10619

[12] Lefkowitz, J. K., Guo, P., Rousso, A., and Ju, Y., "Species and temperature measurements of methane oxidation in a nanosecond repetitively pulsed discharge," *Philos Trans A Math Phys Eng Sci*, Vol. 373, No. 2048, 2015. doi: 10.1098/rsta.2014.0333

[13] Rousso, A., Yang, S., Lefkowitz, J., Sun, W., and Ju, Y., "Low Temperature Oxidation and Pyrolysis of n-Heptane in Nanosecond-pulsed Plasma Discharges," *Proceedings of the Combustion Institute*, Vol. 36, No. 3, 2017, pp. 4105–4112. doi: 10.1016/j.proci.2016.08.084

[14] Ju, Y., Lefkowitz, J. K., Reuter, C. B., Won, S. H., Yang, X., Yang, S., Sun, W., Jiang, Z., and Chen, Q., "Plasma Assisted Low Temperature Combustion," *Plasma Chemistry and Plasma Processing*, Vol. 36, No. 1, 2016, pp. 85–105. doi: 10.1007/s11090-015-9657-2

[15] Yang, S., Gao, X., Yang, V., Sun, W., Nagaraja, S., Lefkowitz, J. K., and Ju, Y., "Nanosecond Pulsed Plasma Activated C2H4/O2/Ar Mixtures in a Flow Reactor," *Journal of Propulsion and Power*, Vol. 32, No. 5, 2016, pp. 1240-1252. doi: 10.2514/1.B36060

[16] Yang, S., Nagaraja, S., Sun, W., and Yang, V., "A Detailed Comparison of Thermal and Nanosecond Plasma Assisted Ignition of Hydrogen-Air Mixtures," *53rd AIAA Aerospace Sciences Meeting*, AIAA Paper 2015-1615, Jan. 2015. doi: 10.2514/6.2015-1615

[17] Zhang, Y., Yang, S., Yang, V., and Sun, W., "Effects of Non-Equilibrium Plasma Discharge on Ignition and NTC Chemistry of DME/O2/Ar Mixtures: A Numerical Investigation," *53rd AIAA/SAE/ASEE Joint Propulsion Conference*, AIAA Paper 2017-4773, Jul. 2017. doi: 10.2514/6.2017-4773

[18] Roettgen, A. M., "Vibrational Energy Distribution, Electron Density and Electron Temperature Behavior in Nanosecond Pulse Discharge Plasmas by Raman and Thomson Scattering," PhD Thesis, *Mechanical Engineering*, The Ohio State University, Columbus, OH, 2015, p. **217**.

[19] Meiden, H. J. v. d., "Thomson scattering on low and high temperature plasmas," PhD, Technische Universiteit Eindhoven, Eindhoven, Netherlands, 2011.

[20] Lefkowitz, J. K., "Plasma Assisted Combustion: Fundamental Studies and Engine Applications," PhD Thesis, *Mechanical and Aerospace Engineering*, Princeton University, Princeton, NJ, 2016.

[21] Farooq, A., Jeffries, J. B., and Hanson, R. K., "In situcombustion measurements of H2O and temperature near 2.5 μm using tunable diode laser absorption," *Measurement Science and Technology*, Vol. 19, No. 7, 2008. doi: 10.1088/0957-0233/19/7/075604

[22] Gordon, I. E., Rothman, L. S., Hill, C., Kochanov, R. V., Tan, Y., Bernath, P. F., Birk, M., Boudon, V., Campargue, A., Chance, K. V., Drouin, B. J., Flaud, J. M., Gamache, R. R., Hodges, J. T., Jacquemart, D., Perevalov, V. I., Perrin, A., Shine, K. P., Smith, M. A. H., Tennyson, J., Toon, G. C., Tran, H., Tyuterev, V. G., Barbe, A., Császár, A. G., Devi, V. M., Furtenbacher, T., Harrison, J. J., Hartmann, J. M., Jolly, A., Johnson, T. J., Karman, T., Kleiner, I., Kyuberis, A. A., Loos, J., Lyulin, O. M., Massie, S. T., Mikhailenko, S. N., Moazzen-Ahmadi, N., Müller, H. S. P., Naumenko, O. V., Nikitin, A. V., Polyansky, O. L., Rey, M., Rotger, M., Sharpe, S. W., Sung, K., Starikova, E., Tashkun, S. A., Auwera, J. V., Wagner, G., Wilzewski, J., Wcisło, P., Yu, S., and Zak, E. J., "The HITRAN2016 molecular spectroscopic database," *Journal of Quantitative Spectroscopy and Radiative Transfer*, Vol. 203, 2017, pp. 3-69. doi: https://doi.org/10.1016/j.jqsrt.2017.06.038

[23] Yang, S., Nagaraja, S., Sun, W., and Yang, V., "Multiscale modeling and general theory of non-equilibrium plasma-assisted ignition and combustion," *Journal of Physics D: Applied Physics*, Vol. 50, No. 43, 2017, p. 433001. doi: 10.1088/1361-6463/aa87ee

[24] Yang, S., Yang, V., Sun, W., Nagaraja, S., Sun, W., Ju, Y., and Gou, X., "Parallel On-the-fly Adaptive Kinetics for Non-equilibrium Plasma Discharges of C2H4/O2/Ar Mixture," *54th AIAA Aerospace Sciences Meeting*, AIAA Paper 2016-0195, Jan. 2016. doi: 10.2514/6.2016-0195

[25] Hagelaar, G., and Pitchford, L., "Solving the Boltzmann equation to obtain electron transport coefficients and rate coefficients for fluid models," *Plasma Sources Science and Technology*, Vol. 14, No. 4, 2005, pp. 722-733.

[26] Kulikovsky, A., "A more accurate Scharfetter-Gummel algorithm of electron transport for semiconductor and gas discharge simulation," *Journal of computational physics*, Vol. 119, No. 1, 1995, pp. 149-155.

[27] Wang, W., Berthelot, A., Zhang, Q., and Bogaerts, A., "Modelling of plasma-based dry reforming: how do uncertainties in the input data affect the calculation results?," *Journal of Physics D: Applied Physics*, Vol. 51, No. 20, 2018, p. 204003.

[28] Martens, T., Bogaerts, A., Brok, W., and van Dijk, J., "Computer simulations of a dielectric barrier discharge used for analytical spectrometry," *Analytical and bioanalytical chemistry*, Vol. 388, No. 8, 2007, pp. 1583-1594.